

## Mechanical Properties of Ultra-High Molecular Weight Polyethylene Irradiated with Gamma Rays

Choon Soo Lee, Seung Hoo Yoo, and Jae Young Jho\*

*Hyperstructured Organic Materials Research Center and School of Chemical Engineering,  
Seoul National University, Seoul 151-744, Korea*

Kuiwon Choi

*Biomedical Research Center, Korea Institute of Science and Technology, Seoul 136-791, Korea*

Tae-Won Hwang

*Research and Development Division for Hyundai Motor Company and Kia Motors Corporation, Kyunggi 445-850, Korea*

*Received Oct. 27, 2003; Revised Jan. 6, 2004*

**Abstract:** With the goal of enhancing the creep resistance of ultra-high molecular weight polyethylene (UHMWPE), we performed gamma irradiation and post-irradiation annealing at a low temperature, and investigated the crystalline structures and mechanical properties of the samples. Electron spin resonance spectra reveal that most of the residual radicals are stabilized by annealing at 100 °C for 72 h under vacuum. Both the melting temperature and crystallinity increase after increasing the dose and by post-irradiation annealing. When irradiated with the same dose, the quenched sample having a higher amorphous fraction exhibits a lower swell ratio than does the slow-cooled sample. The measured tensile properties correlate well to the crystalline structure of the irradiated and annealed samples. For enhancing creep resistance, high crystallinity appears to be more critical than a high degree of crosslinking.

**Keywords:** polyethylene, ultra-high molecular weight, irradiation, annealing, mechanical property, creep.

### Introduction

Ultra-high molecular weight polyethylene (UHMWPE) has been used as a substitute for damaged or diseased cartilage in total joint prosthesis for many years.<sup>1,2</sup> Beside its superb wear resistance, the good mechanical property, chemical resistance, and biocompatibility were the factors that ensure the extensive use of UHMWPE. Cases indicating problems associated with the material, however, have been reported in recent years. The primary problem is the constant generation of submicron-sized wear debris, which limits the service life of prosthesis. Many efforts have been made to enhance the wear resistance of UHMWPE, and crosslinking the chains by chemical reagents or irradiation was one of such efforts.

In fact irradiation with gamma rays is the common practice to sterilize UHMWPE prosthesis. Upon gamma irradiation, following the formation of free radicals, chain scission as well as crosslinking occurs.<sup>3-10</sup> During shelf storage or *in vivo*, residual radicals react with oxygen diffusing from the

surface, which generates peroxy radicals. The peroxy radicals continue to react over the period of years to lead to oxidative degradation.<sup>3,4</sup> While the crosslinking contributes to the enhancement of resistance to wear and creep, the oxidative chain scission deteriorates material properties. Hence, irradiation or post-irradiation heat treatment under an oxygen-free atmosphere is required.<sup>2,5,6</sup>

Since the late 1990s a group of new prostheses with enhanced wear and oxidation resistance have been introduced.<sup>2,5,6</sup> They utilize gamma irradiation and post-irradiation remelting at temperatures above the melting temperature to stabilize the residual radicals remaining mainly in the crystalline region. However, heat treatment at such a high temperature may result in the decrease in crystallinity and creep resistance, which is also important for the longevity of prosthesis material, and consequently reduce the positive effect of irradiation-induced crosslinking. In the present study, we investigate the effect of post-irradiation annealing at a temperature below melting temperature on the mechanical properties of UHMWPE. Electron spin resonance technique was used in order to examine the effect of post-irradiation annealing on the radical stabilization. Structural parameters

\*e-mail: jjho@snu.ac.kr

1598-5032/02/112-07©2004 Polymer Society of Korea

including melting temperature, crystallinity, lamellar thickness, long spacing, and swell ratio were determined. Tensile and tensile creep tests were carried out for the samples prepared by systematically varying gamma irradiation dose and thermal history.

## Experimental

**Materials and Sample Preparation.** UHMWPE used in this study was GUR 4120 from Ticona with the reported weight average molecular weight of  $5 \times 10^6$  g/mol. The powder UHMWPE was compression molded at 200°C for 15 min to form the sheet samples of 1 mm thickness. The molten samples were either slowly cooled to ambient temperature as spaced between the mold plates or quenched between two stainless steel plates pre-chilled at -20°C. Gamma ray irradiation was performed at room temperature in a nitrogen atmosphere using a cobalt-60 source. Total doses were 10, 50, and 100 kGy, and the dose rate was 7.5 kGy/h. The irradiated samples were annealed at 100°C for 72 h in a vacuum oven in order to stabilize the residual radicals.

**Characterization.** Electron spin resonance (ESR) measurements were done at room temperature on a Bruker ESP 300 EPR spectrometer operating at 9.7 GHz microwave frequency. The amplitude of the microwave power was maintained at 20 mW, and the field-modulation amplitude was 10.4 Gauss. As the purpose of ESR measurements was to verify if radicals still existed after annealing, quantitative analysis was not performed. Differential scanning calorimetry (DSC) was performed using a TA Instruments DSC 2920 under a nitrogen atmosphere at a heating rate of 10°C/min. Melting temperature and degree of crystallinity were determined during the heating scan. Small angle X-ray scattering (SAXS) measurements were conducted using the beamline BL4C1 at the Pohang Accelerator Laboratory.<sup>11</sup> The wavelength of the X-ray beam was 1.607 Å. A Princeton CCD area detector placed at a distance of 3.2 m from the sample was used to detect the scattered X-rays. Lamellar thickness and long spacing were determined via the one-dimensional correlation function method.<sup>7,12</sup> Swelling measurements of the irradiated samples were conducted according to a previously reported method.<sup>13</sup> The sol-fraction was extracted for 72 h using boiling *p*-xylene including 0.5 wt% of an antioxidant, 2,6-di-*t*-butyl-4-methyl phenol. After extraction, the gel was transferred to fresh *p*-xylene and allowed to equilibrate at 120°C for 2 h. The swollen gel was then quickly transferred to a weighing bottle, covered, and weighed. The samples were then deswollen in acetone for 24 h and dried at 60°C in a vacuum oven. The swell ratio was determined from the weight ratio of the swollen gel to the dried extracted gel.

**Mechanical Testing.** Dog-bone type tensile specimens were stamped using a cutting die out of 1 mm thick sheets into the geometry conforming to ASTM D638 type V. Using

a Lloyd LR-10K universal testing machine, tensile tests were carried out at room temperature with a crosshead speed of 50 mm/min. Nine tests were performed for each sample. Tensile creep tests were performed at room temperature using a TA Instruments DMA 2980 in the creep mode. A tensile load corresponding to the stress of 5 MPa was applied for 1200 min to the specimen of a dimension 3 mm  $\times$  20 mm  $\times$  1 mm. Strain recovery was also monitored for 1200 min after removing the applied load.

## Results and Discussion

**Crystalline Structure.** DSC heating thermograms are shown in Figure 1, and the results of structure characterization for the samples are listed in Table I. In general, the crystallinity of the samples is lower than that of high density polyethylenes, which is the result of the high degree of entanglements and consequent randomly arranged lamellar morphology in UHMWPE.<sup>2,14</sup> Peak melting temperature ( $T_m$ ), degree of crystallinity ( $X_c$ ), lamellar thickness ( $l_c$ ), and long spacing ( $L$ ) are all larger for the slow-cooled sample (SN0) than the quenched sample (QN0), which indicates that the slow cooling rate produced more perfect and thicker lamellae. The increases in the parameters of QA0 and SA0 from those of QN0 and SN0, respectively, are attributed to lamellar thickening and/or perfection by annealing.

Figure 2 shows the ESR spectra for the slow-cooled UHMWPEs. Little difference was found between the spectra for the slow-cooled and the quenched samples. Septet peaks indicating allyl radicals with some alkyl and polyenyl radicals

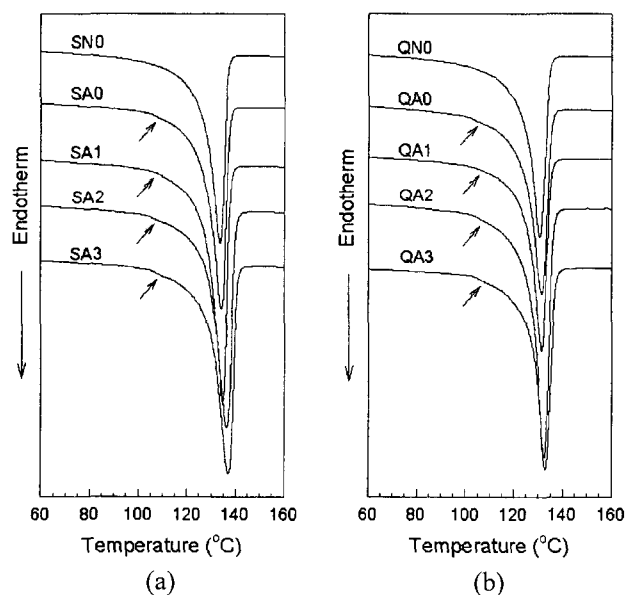


**Figure 1.** DSC heating thermograms of (a) slow-cooled and (b) quenched UHMWPEs. The arrows indicate the position of the weak shoulders.

**Table I. Structural Characteristics of UHMWPEs Measured from DSC, SAXS, and Swelling Measurements**

Sample Code <sup>a</sup>	Sample Processing	Irrad. Dose (kGy)	$T_m$ (°C)	$X_c$ (%)	$l_c$ (nm)	$L$ (nm)	Swell Ratio
SN0	slow cooling	0	133.7	48.7	21.8	42.0	-
SN1	slow cooling	10	134.4	50.5	-	-	18.2
SN2	slow cooling	50	135.7	51.8	-	-	5.8
SN3	slow cooling	100	137.4	51.5	-	-	4.9
SA0	slow cooling	0	134.3	51.9	21.9	43.0	-
SA1	slow cooling	10	134.9	54.4	22.4	40.5	18.1
SA2	slow cooling	50	135.9	56.6	21.5	38.5	5.2
SA3	slow cooling	100	137.6	56.2	21.9	38.5	3.9
QN0	quenching	0	129.8	43.7	16.7	33.0	-
QN1	quenching	10	130.5	44.3	-	-	11.0
QN2	quenching	50	132.4	46.9	-	-	4.8
QN3	quenching	100	132.6	49.1	-	-	3.9
QA0	quenching	0	131.4	46.0	20.7	39.0	-
QA1	quenching	10	131.4	50.3	19.5	36.5	10.6
QA2	quenching	50	132.4	51.2	18.5	32.0	4.4
QA3	quenching	100	132.6	52.9	18.5	31.0	3.2

<sup>a</sup>Character N and A in the codes denote the samples not-annealed and annealed, respectively.

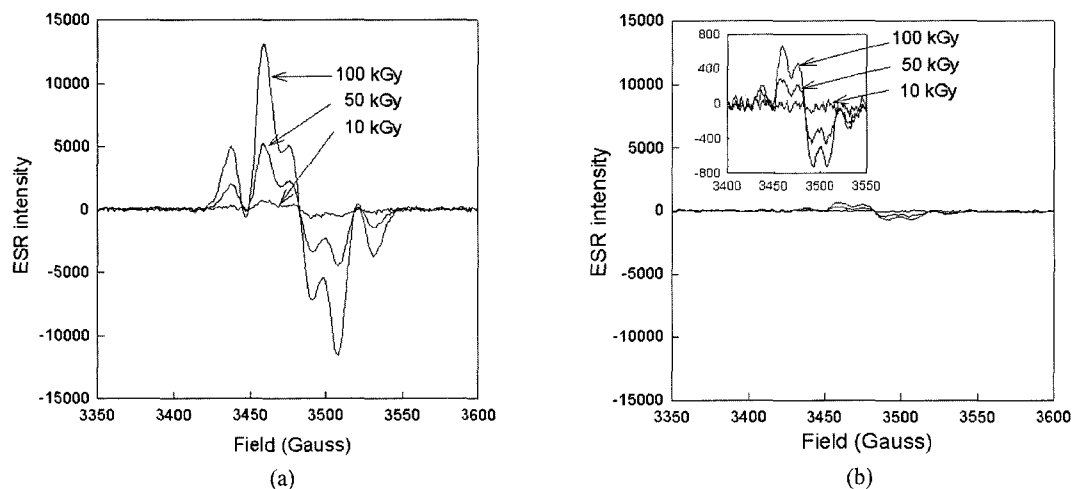


**Figure 2.** ESR spectra of irradiated UHMWPEs: (a) as irradiated and (b) after post-irradiation annealing. The inset of (b) shows that the spectral shape is not changed by the post-irradiation annealing.

were observed in the spectra of the as-irradiated samples as shown in Figure 2(a).<sup>4</sup> Most radicals produced in the crystalline region upon gamma irradiation still remain due to the low mobility of the chains at room temperature. Upon post-irradiation annealing, ESR intensities are substantially reduced with overall spectral shape unchanged, indicating that a large portion of residual radicals are stabilized with little oxidation in the process of annealing under vacuum. For the complete stabilization of the residual radicals, heat

treatment under the condition of a higher temperature and a longer annealing time appears to be required.

As shown in Table I, swell ratio, which inversely reflects the extent of crosslinking, decreases with increasing dose of gamma ray, and is smaller for the quenched sample than the slow-cooled sample irradiated with the same dose. It indicates that the doses chosen in this study effectively induce the crosslinking of the chains in the amorphous region of UHMWPE.<sup>8</sup> It is also observed that swell ratio decreases a

little upon annealing, indicating that further crosslinking proceeds via the combination of the residual radicals during post-irradiation annealing.

The effect of irradiation on the crystalline structure of UHMWPE is rather complex.  $T_m$  increases with increasing irradiation dose and by post-irradiation annealing. Although the high  $T_m$  usually is the indication of thick lamellae,<sup>15</sup> the lamellae of the irradiated annealed sample in the present study, except for SA1, appear thinner than those of the unirradiated annealed sample. It is thought that the irradiation-induced crosslinks hinder the lamellar thickening in the annealing step by lowering the mobility of chains in the amorphous and interfacial region. The crosslinks also result in the higher  $T_m$  of the samples irradiated with higher dose by kinetically arresting the melting process.<sup>7</sup> The higher  $l_c$  of SA1 compared to that of unirradiated sample (SA0) is considered to be the result of lamellar thickening by annealing, which was less hindered due to the low degree of crosslinking.

The increase in  $X_c$  with irradiation dose and by annealing can be explained by crystal perfection and formation of new crystals during annealing. In addition to crosslinking, chain scission also occurs upon gamma irradiation, and these two processes progress to a higher degree with increasing dose. It was reported that broken chains are rearranged into the existing crystals, increasing the crystal perfection in as-irradiated UHMWPE.<sup>7,9</sup> In the present study, the post-irradiation annealing promotes such crystal perfection, resulting in the increase in  $X_c$  with irradiation dose. In addition, there is a possibility that the annealing makes the broken chains form new small lamellae in the amorphous region.<sup>7</sup> Lower long spacing for the irradiated samples is due probably to the formation of such new crystals. Weak shoulders, which were observed around 105 °C in the DSC endotherm traces of the annealed samples as shown in Figure 1, support this possibility.

**Tensile Properties.** Figure 3 shows nominal stress-strain curves of the annealed samples compared with those of not-annealed samples. All of the samples show a weak yield drop with a diffuse necking, which develops rather intensively with increasing dose. The apparent degree of the yield drop is higher for the slow-cooled samples than the quenched samples. It is generally known that a large number of entanglements in UHMWPE prevent the transformation of the lamellar to a fibrillar morphology at large deformation,<sup>16,17</sup> which contributes to the early onset of strain hardening. The apparent strain hardening is more intense in the slow-cooled than in the quenched samples. With increasing irradiation dose, the crosslinks promote the strain hardening right after yielding. During deformation the increased number of crosslinks can withstand a higher stress, resulting in the higher degree of strain hardening.

SA0 and QA0 show significant reductions in elongation at break compared with SN0 and QN0, respectively. Such

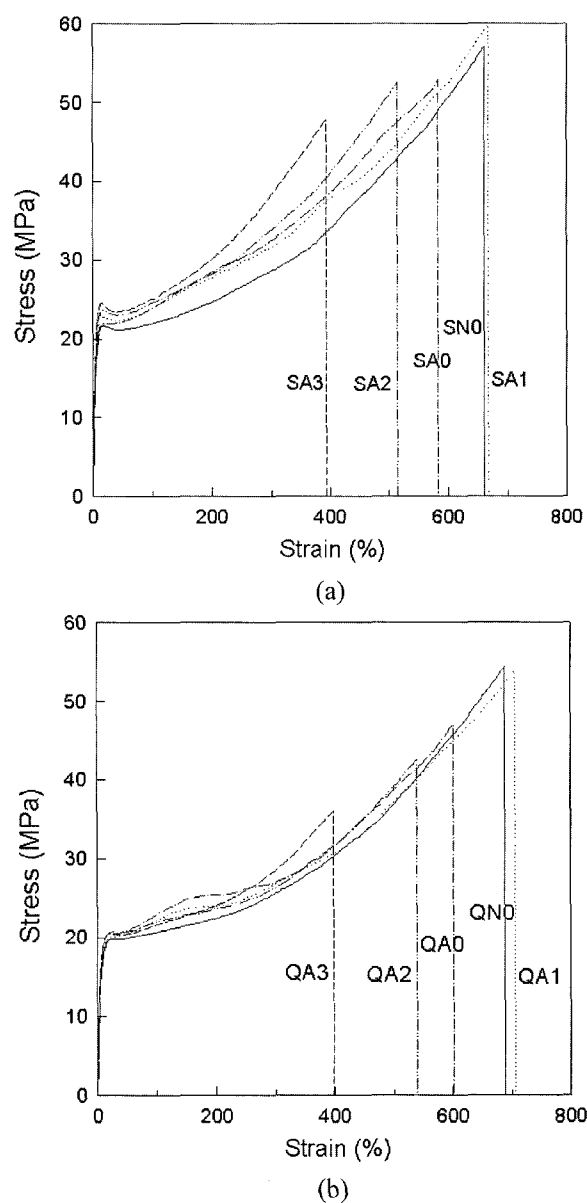


**Figure 3.** Stress-strain curves of (a) slow-cooled and (b) quenched UHMWPEs.

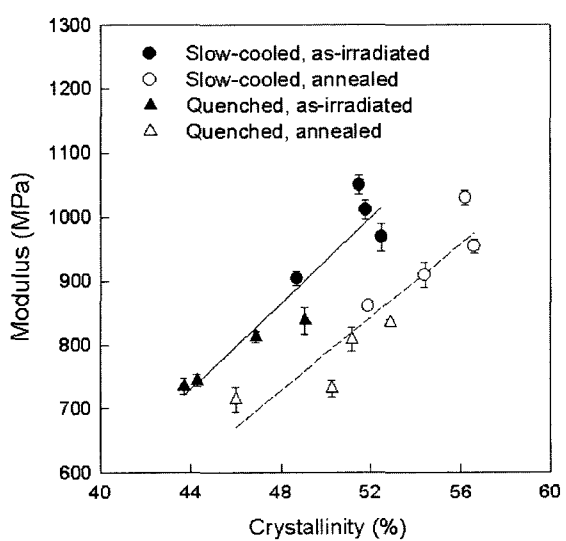
reduced deformability of the annealed samples may be associated with the lamellar surface that is highly stressed via the refolding process during annealing at 100 °C. The samples irradiated with high doses of 50 and 100 kGy fail at lower elongation at break than unirradiated samples do. It appears that the crosslinks induced inhibit chain orientation along the tensile direction and consequently promote the material failure. However, SA1 and QA1 show no decrease in the elongation at break compared with the untreated samples, SN0 and QN0, respectively. For the samples irradiated with the low dose of 10 kGy, the chain scission outweighing the effect of crosslinking appears to ease deformation at

high strains.

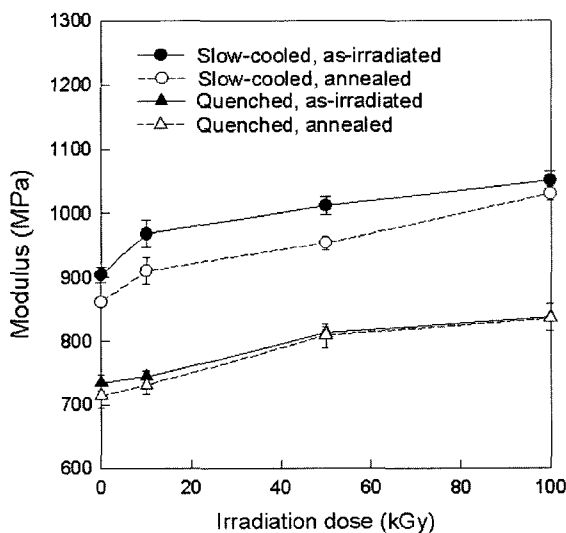
The initial modulus of the annealed and as-irradiated samples is plotted against crystallinity and irradiation dose in Figure 4. As initial elastic deformation is mainly associated with the deformation of the amorphous region through the processes such as slip, separation, and rotation of lamellae,<sup>18,19</sup> modulus increases with increasing crystallinity as shown in Figure 4(a). In addition to crystallites, crosslinks restrict the deformability of the amorphous region and give rise to the increase in initial modulus as shown in Figure 4(b). A rather unexpected and atypical result is that the modulus of an annealed sample is smaller than that of the as-irradiated sample irradiated at the same dose, in spite of the increased crystallinity of the annealed samples. A credible

explanation for the peculiarity cannot be offered at the present time. As a possible explanation should include significant softening of the amorphous region, extensive disentanglement during annealing and consequent drop in modulus according to the rubber elasticity theory may be one. It has been observed that storage modulus in the melt state<sup>20</sup> and fatigue resistance<sup>21</sup> of polyethylene decline by annealing, which may also be due to disentanglement. However, further investigation appears necessary to comprehend this odd behavior, which has never been reported before.

The yield stress of the samples is plotted against irradiation dose in Figure 5(a). Yield stress is inclined to increase by both of irradiation and annealing, and the slow-cooled samples show higher yield stresses than the quenched sam-

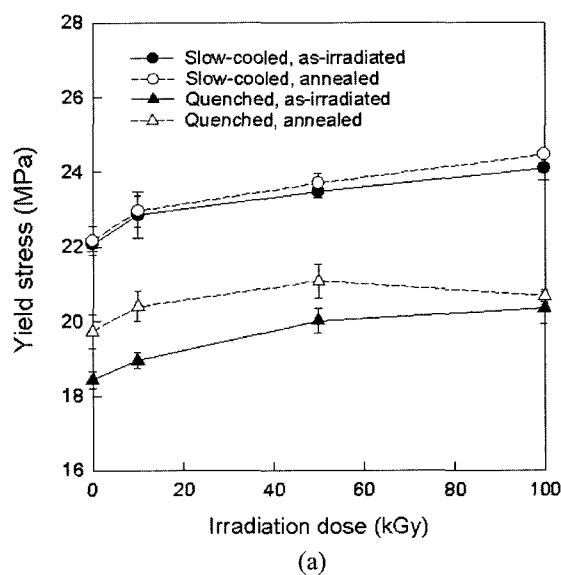


(a)

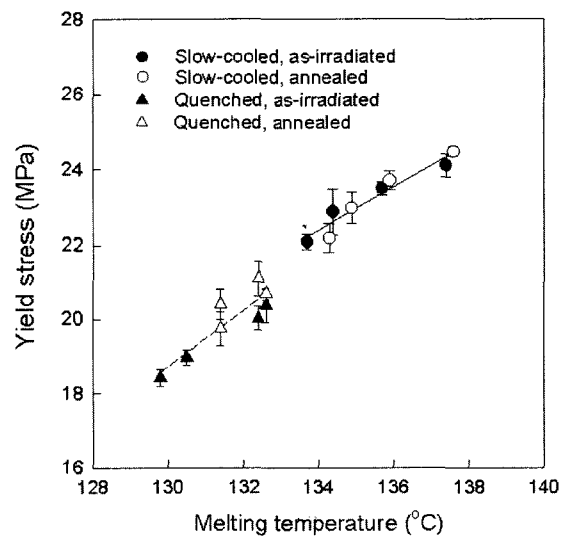


(b)

**Figure 4.** Plot of initial modulus against (a) crystallinity and (b) irradiation dose.



(a)



(b)

**Figure 5.** Plot of yield stress against (a) irradiation dose and (b) melting temperature.

ples. It is generally recognized that lamellar thickness mainly influences the magnitude of yield stress.<sup>22</sup> Crosslinks, acting as the obstacle to lamellar chain slip, can also increase yield stress. For the irradiated samples, as mentioned above, the melting point reflects the effects of crosslinks in addition to lamellar thickness. Hence, yield stresses are well correlated with melting point as shown in Figure 5(b).

**Creep Behavior.** As high resistance to creep, in addition to general mechanical properties, is a requisite for the prosthesis material, tensile creep and recovery behavior of the samples was examined. The samples were subjected to a static tensile stress of 5 MPa for 1200 min and subsequently let recovered for another 1200 min right after unloading. Figure 6 shows the tensile creep and recovery curves of annealed samples as compared to untreated samples, SN0 and QN0. The creep

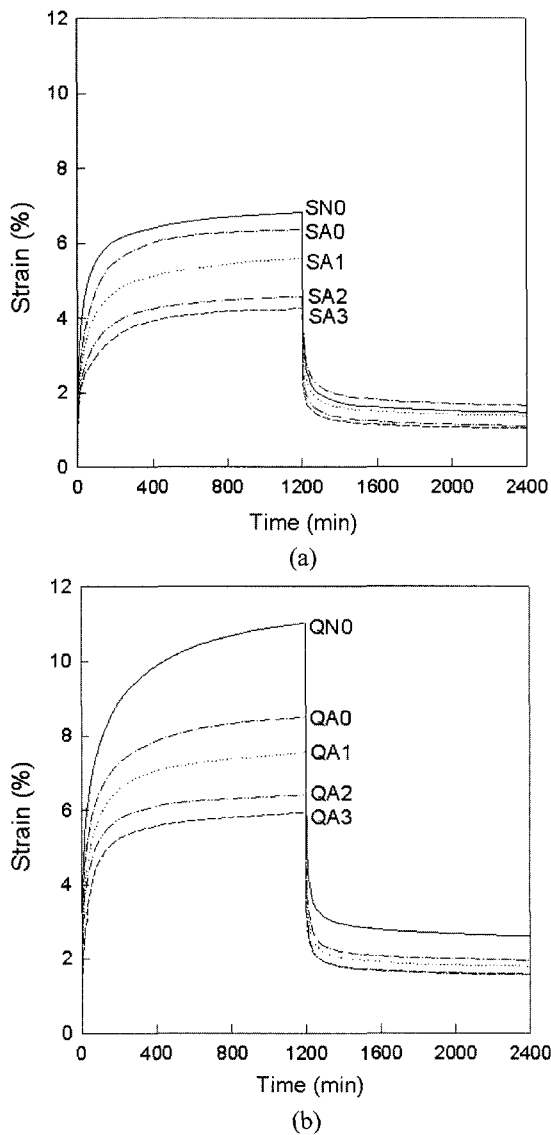


Figure 6. Tensile creep and recovery curves of (a) slow-cooled and (b) quenched UHMWPEs.

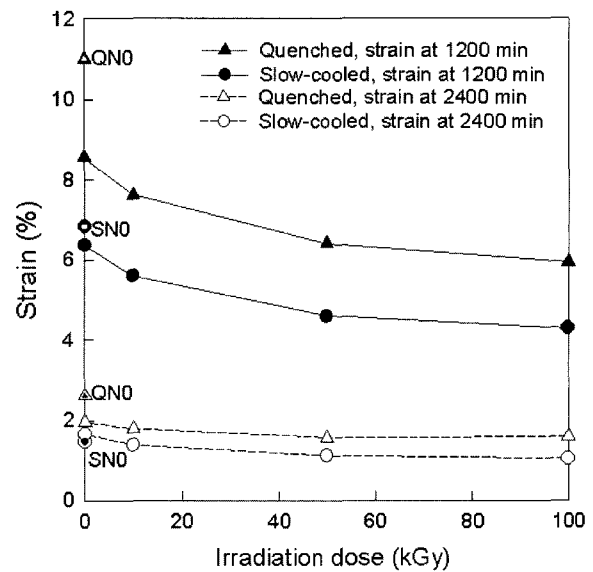


Figure 7. Creep strain and residual strain of UHMWPEs.

strain at 1200 min and the residual creep at 1200 min after unloading are plotted against irradiation dose in Figure 7. Creep is a long-term deformation concomitant with the gradual release of local stress in the sample by short-range molecular rearrangement under the stress applied at the level lower than yield stress. Chain slip is less susceptible to occur in high-crystallinity samples with thick lamellae compared to low-crystallinity samples. As a result, the slow-cooled samples reveal relatively low creep strains compared to the quenched samples. It is also observed that the irradiation and post-irradiation annealing improves creep resistance. Crosslinks in the amorphous region appear to constrain the chain slip effectively.

The residual deformation at 1200 min after unloading is inclined to decrease as the irradiation dose increases, which is the result of enhanced creep resistance by increased crosslinks. It is, however, observed that both of the creep strain and the residual strain of the quenched sample are larger than those of the slow-cooled sample at the same irradiation dose, despite the higher crosslinking density of the quenched sample. It can be attributed to the lower crystallinity in the quenched sample. While both of high crystallinity with thick lamellae and crosslinks in the amorphous region are beneficial for high creep resistance, it appears that crystallinity is more influential than crosslinking. It is therefore concluded that, post-irradiation heat treatment at temperatures lower than the melting temperature is favored over post-irradiation remelting, which should reduce crystallinity of the material.<sup>2,5,6</sup>

## Conclusions

Crystalline structure and mechanical properties including

creep resistance were investigated for the UHMWPEs that were gamma-irradiated and heat-treated at a temperature lower than the melting temperature. ESR analysis ascertains that most of residual radicals are stabilized by the annealing. When irradiated with the same dose, the quenched sample with higher amorphous fraction shows a lower swell ratio than the slow-cooled sample. The irradiation-induced crosslinks contribute to the high melting temperature of the irradiated UHMWPE. Post-irradiation annealing promotes the increase in crystallinity via crystal perfection. The tensile tests reveals that crosslinks play a major role in enhancing the strain hardening and in reducing the elongation at break. The initial modulus is well correlated to the crystallinity, and the yield stress is well correlated to the melting temperature, reflecting the effects of the lamellar thickness and crosslinks. While creep resistance is enhanced with both of crystallinity and degree of crosslinking, high crystallinity appears more important than crosslinks.

**Acknowledgements.** This work was supported partly by Korean Ministry of Health and Welfare (98-PJ7-PG4-2-0054) and partly by Korea Science and Engineering Foundation through the Hyperstructured Organic Materials Research Center. SAXS experiments at PLS were supported in part by MOST and POSTECH.

## References

- (1) G. Lewis, *J. Biomed. Mater. Res.*, **38**, 55 (1997).
- (2) S. M. Kurtz, O. K. Muratoglu, M. Evans, and A. A. Edidin, *Biomaterials*, **20**, 1659 (1999).
- (3) B. Yeom, Y. -J. Yu, H. A. McKellop, and R. Salovey, *J. Polym. Sci., Polym. Chem. Ed.*, **36**, 329 (1998).
- (4) M. S. Jahan, M. C. King, W. O. Haggard, K. L. Sevo, and J. E. Parr, *Radiat. Phys. Chem.*, **62**, 141 (2001).
- (5) H. McKellop, F. Shen, B. Lu, P. Campbell, and R. Salovey, *J. Orthop. Res.*, **17**, 157 (1999).
- (6) R. Chiesa, M. C. Tanzi, S. Alfonsi, L. Paraccjini, M. Moscatelli, and A. Cigada, *J. Biomed. Mater. Res.*, **50**, 381 (2000).
- (7) V. Premnath, A. Bellare, E. W. Merrill, M. Jasty, and W. H. Harris, *Polymer*, **40**, 2215 (1999).
- (8) P. H. Kang and Y. C. Nho, *Radiat. Phys. Chem.*, **60**, 79 (2001).
- (9) S. K. Bhateja, R. W. Duerst, J. A. Martens, and E. H. Andrews, *J. Macromol. Sci. R.M.C.*, **C35**, 581 (1995).
- (10) C. Birkinshaw, M. Buggy, S. Daly, and M. O'Neill, *J. Appl. Polym. Sci.*, **38**, 1967 (1989).
- (11) J. Bolze, J. Kim, J.-Y. Huang, S. Rah, H. S. Youn, B. Lee, T. J. Shin, and M. Rhee, *Macromol. Res.*, **10**, 2 (2002).
- (12) G. R. Strobl and M. J. Schneider, *J. Polym. Sci., Polym. Phys. Ed.*, **18**, 1343 (1980).
- (13) A. P. de Boer and A. J. Pennings, *J. Polym. Sci., Polym. Phys. Ed.*, **14**, 187 (1976).
- (14) J. Maxfield and L. Mandelkern, *Macromolecules*, **10**, 1141 (1977).
- (15) U. W. Gedde, *Polymer Physics*, Chapman & Hall, New York, 1995, chapter 7.
- (16) W. Wilke and M. Bratrich, *J. Appl. Cryst.*, **24**, 645 (1991).
- (17) M. F. Butler, A. M. Donald, and A. J. Ryan, *Polymer*, **39**, 39 (1998).
- (18) L. Lin and A. S. Argon, *J. Mater. Sci.*, **29**, 294 (1994).
- (19) M. A. Kennedy, A. J. Peacock, and L. Mandelkern, *Macromolecules*, **27**, 5297 (1994).
- (20) C. S. Lee, J. Y. Jho, K. Choi, and T.-W. Hwang, *Macromol. Res.*, submitted.
- (21) J. J. Strebel and A. Moet, *J. Polym. Sci., Part B: Polym. Phys.*, **33**, 1969 (1995).
- (22) N. W. Brooks and M. Mukhtar, *Polymer*, **41**, 1475 (2000).